

Molecular Physics

An International Journal at the Interface Between Chemistry and Physics

ISSN: 0026-8976 (Print) 1362-3028 (Online) Journal homepage: <http://www.tandfonline.com/loi/tmph20>

Quantitative study of diffusion jumps in atomistic simulations of model gas-polymer systems

Theophanes E. Raptis , Vasilios E. Raptis & Jannis Samios

To cite this article: Theophanes E. Raptis , Vasilios E. Raptis & Jannis Samios (2012) Quantitative study of diffusion jumps in atomistic simulations of model gas-polymer systems, Molecular Physics, 110:11-12, 1171-1178, DOI: [10.1080/00268976.2012.663511](https://doi.org/10.1080/00268976.2012.663511)

To link to this article: <http://dx.doi.org/10.1080/00268976.2012.663511>



Accepted author version posted online: 09 Feb 2012.
Published online: 27 Feb 2012.



Submit your article to this journal [↗](#)



Article views: 103



View related articles [↗](#)



Citing articles: 1 View citing articles [↗](#)

INVITED ARTICLE

Quantitative study of diffusion jumps in atomistic simulations of model gas–polymer systems

Theophanes E. Raptis^a, Vasilios E. Raptis^b and Jannis Samios^{c*}

^aDivision of Applied Technology, NCSR “Demokritos”, GR-153 10 Athens, Greece; ^bDepartment of Materials Science and Engineering, University of Ioannina, GR-451 10 Ioannina, Greece; ^cDepartment of Chemistry, Laboratory of Physical and Theoretical Chemistry, University of Athens, Panepistimiopolis GR-157 7, Athens, Greece

(Received 15 November 2011; final version received 27 January 2012)

Microscopic mechanisms underlying the diffusion of particles in polymeric and other systems include ‘jumps’ that are said to provide for a substantial contribution to the overall particle displacement. Such jumps have been observed in molecular simulations and experimentally, leading to important qualitative conclusions. An efficient method has been proposed for the identification and quantitative processing of jumps, and successfully employed in simulations of gas–liquid alkane systems. In the present work, the same method is applied in equilibrium Molecular Dynamics simulations of methane-like molecules dispersed in polymer-like alkanes, at atmospheric pressure and temperature well above the polymer melting point. The systems studied were prepared and equilibrated and a linear diffusion regime was confirmed by means of various criteria. The occurrence of distinct jump events was clearly revealed and their average length and frequency were calculated. In this way, a random-walk-type diffusion coefficient, $D_{s,jumps}$, of the penetrants, was obtained and found to be lower than the overall diffusion coefficient $D_{s,MSD}$ calculated by the mean square displacement method. This is a strong indication that the overall diffusion is a combination of longer jumps with other microscopic mechanisms such as smoother and more gradual displacements effected upon the diffusing particle by its surroundings.

Keywords: molecular dynamics; molecular simulation; diffusion; penetrant jumps; macromolecular systems

1. Introduction and general considerations

Jumps of diffusing microscopic particles play an important role in diffusion theory and have been observed in both molecular simulations and experimental studies [1, 2]. Once a particle’s trajectory is recorded and plotted, it is often easy to identify such jumps, although their quantitative processing based on raw numerical data would require a more elaborate technique. A computational technique of this kind has been proposed and its efficiency has been demonstrated in Molecular Dynamics (MD) simulations of gaseous hydrocarbon molecules dispersed in heavier liquid alkanes [3]. The contribution of jumps to the overall diffusion was shown to be rather small, thus indicating their co-existence with other transport mechanisms such as gradual displacement. It would be of interest to investigate whether this conclusion holds also for systems of larger chain molecules in the liquid state or if the jumps actually constitute the main mechanism of diffusion in that case. Thus, at this point we have to mention that, in the present work, we decided to extend previous studies in the field in order to explore systematically the aforementioned questions.

Indeed, several studies have implied that such jumps might play a prominent role in the translocation of small molecules through polymeric matrices [4–26]. While this may be true regarding ‘fixed’ systems of polymers in the glassy state, one might expect different behavior when studying liquid systems. The synergistic motion of neighboring polymer segments may result in a continuous drifting motion of the penetrants, co-existing with more or less abrupt displacements that can be identified as jump events. The concept of a jump event is an idealized one; it is often employed because of its appealing similarity with the random-walk model. On the other hand, attempted descriptions of diffusion jumps in amorphous liquid matrices are rather vague. Usually, one considers a small particle to be trapped in some form of cavity of randomly changing shape and size due to thermal fluctuations. When thermal motion allows a ‘tunnel’ to be temporarily formed between the host cavity and another, nearby one, the trapped penetrant might percolate to that neighboring empty site. This is said to be a jump event.

At the same time, a jump is thought of as something ‘sharp’ and fast, resulting in a displacement

*Corresponding author. Email: isamios@chem.uoa.gr

that is longer than the average. The random inter-cavity percolation motion just described does not necessarily resemble this picture. What is more, there might even be instances where the penetrant returns to the initial host cavity – if the latter still exists. These ‘come-back’ events do not contribute significantly to the overall diffusion motion and should not be considered as proper jumps. Finally, cavities themselves are neither permanent nor stable or fixed in space. Cavities are topological rather than physical entities and they migrate in a way slightly reminiscent of semiconductor holes, carrying the penetrants with them in a tide-like fashion. This is an example of the drifting motion referred to in the previous paragraph that blurs the beginning and end of an inter-cavity jump.

Diffusion jumps may be identified with thin ‘filaments’ connecting densely populated areas in three-dimensional graphs of penetrant positions or with sharp changes in a plot of displacement versus time. The former method is merely a visualization technique that does not allow for quantitative treatment. Then one is tempted to employ the latter, i.e. use plots of displacement versus time to allow for quantitative processing [5–9, 16–19, 24]. The drawback of the method is its inability to provide for the correct size of a jump. The apparent jump length in such a plot would range from its real value to zero depending on whether the jump took place along the line connecting the original and final penetrant position or at a direction perpendicular to it. To express the displacement as a function of x , y , or z instead of distance from the origin would be too complicated due to the noisy nature of such data sets, requiring additional processing and filtering before further statistical treatment.

More rigorous attempts to study jumps in a quantitative manner include some form of parameterizing an assumed model, relying on a comparison with mean square displacement data, except in Ref. [14] where local orientation correlation functions lead to a spectrum of characteristic length scales. However, the mean square displacement is a measure of the overall diffusion. Using such data to parameterize the jump models assumes implicitly that no diffusion microscopic mechanism other than jumps exist, which is, in general, incorrect as, for instance, suggested by Hahn *et al.* [16]. There, the diffusion of phenol molecules in bisphenol-A-polycarbonate is studied, and a certain coupling of penetrant and local polymer motion is observed, leading to a continuous rather than jump-like displacement.

These methods do provide a picture of penetrant jumps that take place, although they do not, in most cases, provide a rigorous definition of what is a jump.

An efficient definition of diffusive jumps through an amorphous liquid matrix should retain the basic characteristics of ‘sharpness’ and ‘unusually long’ displacement, and at the same time be capable of clearly and unambiguously identifying all events of interest, i.e. the ones that contribute substantially to the overall diffusion. Therefore, instead of trying to rely on ill-defined spatio-temporal characteristics of the trajectory and the penetrant’s environment, one should focus instead on the outcome and devise a descriptor based on the relation of distance travelled within a short period of time. The particle’s velocity averaged over a certain time interval that is to be somehow determined could be such a descriptor. The average velocity would be higher during a jump event, close to zero when the penetrant fluctuates back and forth inside a cavity and have an intermediate value when drifting motion takes place. The occurrence of jump events would then be identified with the location of peaks (local maxima) of the velocity with time curve. However, in the original publication of the method [3] it is mentioned that use of velocity results in a very noisy signal that is impractical to process. A measure of the extent to which successive particle positions are spread in space might provide an easier to handle time series. These positions should occupy a larger and probably elongated volume element during a jump, resulting in a maximum clearly distinct from the background noise.

This is indeed the case for the radius of gyration, R_G , calculated over a set of successive particle positions within an arbitrary time interval. Use of R_G provides an alternative for a precise identification of the diffusion jumps. It is based on tracking the size of the region occupied by a specific number of successive penetrant positions, throughout the simulation. In this way, one can identify all isolated jumps and determine the respective jump lengths. This kind of data can be further processed statistically, leading to information concerning both the average jump length and the frequency of hopping events, provided that a large enough sample has been obtained. With the aid of this information, one can clarify the extent of the contribution of jumps to the overall diffusion and thus elucidate the possible microscopic mechanisms underlying the behavior of diffusion processes in such systems. Finally, it should be noted that the proposed approach is capable of detecting jump events regardless of their origin, i.e. whether the penetrant escaped from a cavity and moved to another one or it was suddenly drawn away due to the matrix’s structural rearrangement or other collective motion.

The present work is organized as follows. In Section 2, the system studied is described, along

with the simulation methodology and the principles and details of the jumps' detection method are provided. In Section 3, the simulation results are presented and discussed. In particular, the simulation trajectory data are processed and information on the jump statistics is obtained and analysed via the method adopted herein. A summary of the main results of our treatment is given in Section 4.

2. Introduction and general considerations

2.1. Simulation details

In the present treatment, a united atom model was employed to study a molecular system of methane-like penetrants dispersed in linear chain molecules of the type $C_{100}H_{202}$, hereafter referred to as 'heavy substance', 'liquid' or 'polymer'. The last term is justified by the fact that the chain molecule's weight exceeds the polyethylene entanglement molecular weight (~ 1200) [27]. The system under study was simulated by means of the equilibrium MD simulation technique three times independently, starting each time from a different initial system configuration properly constructed. These simulations are a preliminary step of wider research, currently under way, that will entail the investigation of microscopic mechanisms underlying diffusion through linear and branched macromolecules of various molecular weights. The penetrant gases are chemically similar to the heavier substances, and therefore interference by other factors such as molecular architecture and chemical composition is almost eliminated. The force-field was based on the well-known NERD [28] and UA-TrAPPE [29] models, in which both CH_2 and CH_3 groups are represented as single interaction sites. Details about the model and the parameters employed are the same as in Ref. [3].

As mentioned above, three initial configurations were constructed at a density equal to 0.73 g cm^{-3} , i.e. somewhat lower than that of amorphous polyethylene at its melting point and atmospheric pressure [30]. All such structures contained 1000 united atoms of the heavy substance, i.e. 10 polymeric liquid molecules, and 20 penetrant molecules of the diffusing substance (methane). The gas molecules were uniformly dispersed in the systems, thanks to the sample construction method, as explained in the next paragraph, a fact that was confirmed by visual inspection of the initial configurations.

The method of creating the initial samples is the same as in the original publication of the method [3] and has been described in detail therein. In brief, cubic periodic boundary conditions were imposed, all gaseous molecules and the first atom of each polymer were

randomly placed in the simulation box, and then the polymer molecules were built in a step-wise fashion, by adding one new bond to each molecule at every step. Bond orientations were chosen, among a discrete set of trial directions, using a Metropolis energetic criterion and configurations with strongly overlapping non-bonded atom pairs were excluded. A diameter of 2.5 \AA was employed for all united atoms. This stage allowed for a reasonable distribution of torsion angles, which is essential for constructing realistic amorphous samples. Then, energy optimization followed by slightly displacing randomly chosen atoms in a Monte Carlo like fashion. The process consisted of consecutive MC cycles with gradually increasing atomic diameters up to their normal values given by the force-field. The structure relaxed during each cycle was used as input to the next calculation with larger atomic diameters. Sufficient relaxation was ensured when smooth and diffuse bond angles and dihedral angles' distributions were obtained, instead of the discrete ones imposed during the first stage. The density was held constant throughout the construction and optimization stages.

MD simulations were performed in the isothermal, NVT, statistical mechanical ensemble at a temperature of 450 K, well above the melting point of polyethylene, to ensure that the sample was in the liquid amorphous state. The computations lasted 7 ns; the first nanosecond was considered to be an equilibration stage and was not taken into account in the post-processing computations. In all MD simulations of pure heavy substance and gas mixtures, we utilized the leap-frog Verlet algorithm with a multiple time step of 1 fs for the fast modes and 5 fs for the slow ones. A cutoff distance of 12.5 \AA was adopted for the calculation of Lennard-Jones interactions. All simulations were performed with the Nosé-Hoover method for the NVT ensemble.

Sufficient equilibration of the systems was ensured by certain criteria such as change of potential energy with time, running average of the density and torsion angles' distribution and decorrelation with respect to the original structure. In particular, the total and Lennard-Jones potential energy were observed to decrease during the first 100 ps and then to keep fluctuating about a constant value. This is an indication that residual overlaps among the various interaction sites, which escaped the equilibration stage during the initial structure generation process, were easily removed during the MD simulation. The other components also exhibited the same fluctuating behavior from the very beginning. The running average of the systems density reached an asymptotic value within the first 1 ns of the simulations. Furthermore, by dividing

the simulation cell into eight equal sub-boxes recording the number density running average in each of them, it was observed that the corresponding values differed by less than 1% within the first 1 ns equilibration period. The dihedral angles' distribution recorded during each one of the first five nanoseconds (ns) of the simulations was virtually identical to the one obtained by the building procedure which ensures generation of amorphous structures. The dihedrals time autocorrelation function, as described in Ref. [3], was also computed and revealed loss of structural memory within the first nanosecond. It was thus ensured that the systems were not frozen in their initial state but were actually liquid.

2.2. Jumps detection method – Diffusion mechanisms

Details of the identification of jumps and processing procedure can be found in Ref. [3]. Here, the basic principles are briefly reviewed and then the practicalities of the implementation are discussed. To devise the method, it was assumed that the penetrant particle spends its 'life' inside various free volume cavities formed by the heavy substance matrix, interrupted by small time intervals when thermal fluctuations allow the molecule to jump from one cavity to another. Thus, by recording its centre-of-mass position N times within a time interval Δt , we collect a swarm of points that is usually concentrated inside a particular area but becomes elongated when a jump occurs. Of course, a similar effect is to be expected in the case of a penetrant moving from one end of an elongated cavity to the other. It should be stressed that the present approach is not about the polymeric environment but rather about the penetrant trajectory itself. Therefore, it is not restricted to such systems but it is actually more generic and applicable whenever jump-like behavior occurs. Indeed, Zheng *et al.* [2] relied on the approach employed here to study the Brownian-like motion of gold nanoparticles dispersed in thin water–glycerol films, based on experimental data obtained by Transmission Electron Microscopy.

The swarm size as a function of time is given by the radius of gyration, R_G , taken over all swarm points

$$R_G(t; \Delta t) = \sqrt{\frac{1}{N} \sum_{i=1}^N (\mathbf{R}_i(t; \Delta t) - \mathbf{R}_{CM}(t; \Delta t))^2}, \quad (1)$$

where time t denotes the middle of the observation time interval Δt , $\mathbf{R}_i(t; \Delta t)$ is the position of every observation point and \mathbf{R}_{CM} is the swarm center-of-mass. The jump length is then defined in two ways. The *unweighted* jump length $\lambda'(t; \Delta t)$ is

given by

$$\lambda'(t; \Delta t) = 2R_G(t; \Delta t), \quad (2)$$

which is actually the width of a three-dimensional normal distribution of the swarm points centered at \mathbf{R}_{CM} , with a variance equal to the radius of gyration (Equation (1)). This is justified by the fact that diffusion jumps are complicated events that themselves constitute a random walk [3].

The *weighted* jump length is given by the relation:

$$\begin{aligned} \lambda(t) &= 2R_G(t; \Delta t) \frac{\|\mathbf{R}_1(t; \Delta t) - \mathbf{R}_N(t; \Delta t)\|}{\sum_{i=1}^{N-1} \|\mathbf{R}_i(t; \Delta t) - \mathbf{R}_{i+1}(t; \Delta t)\|} \\ &= \lambda'(t; \Delta t) \frac{\|\mathbf{R}_1(t; \Delta t) - \mathbf{R}_N(t; \Delta t)\|}{\sum_{i=1}^{N-1} \|\mathbf{R}_i(t; \Delta t) - \mathbf{R}_{i+1}(t; \Delta t)\|}. \end{aligned} \quad (3)$$

The numerator is the distance r_{1N} or the 'end-to-end' vector of the swarm, and the denominator is the contour length of the path defined by the N recorded positions. Their ratio accounts for the fact that certain jumps might be 'unsuccessful', i.e. the penetrant might return to its original position. For an 'ideal' jump, this ratio would approach unity, otherwise it would be smaller.

Interestingly, it was pointed out [3] that the weighted jump tends to a constant value with increasing Δt , thus solving the problem of using an arbitrary parameter. One then has to perform calculations for increasing time intervals and retain the *weighted* jump size obtained at long enough Δt , usually no more than 150 ps. Then, by considering the series of jumps observed as a random walk, one can define a corresponding diffusion coefficient, $D_{s,jumps}$, via the well-known formula [31]

$$D_{s,jumps} = \frac{1}{6} \nu \lambda^2, \quad (4)$$

where ν denotes the frequency of successful jumps and λ the average jump length. In terms of simulation results, the frequency ν is calculated as the number of all successful jumps performed by all the penetrants divided by the total simulation time. The diffusion coefficient, D_s , provides a measure of the contribution of jumps to the overall diffusive motion. We may state that the contribution of jumps to the diffusive motion is important if the respective random-walk diffusivity is close to the mean square displacement one. If, on the other hand, the former is, for example, an order of magnitude lower than the latter, additional diffusion mechanisms such as smooth translation of the reptation kind should be present.

At this point, it should be noted that the above definitions, Equations (2) and (3), do not measure the

real translation during a specific time interval. That translation is given by the end-to-end vector r_{1N} of the observation points swarm and that is the ‘real’ measure of jump lengths. However, that measure suffers from two drawbacks: it provides very noisy signals that are hard to process and it is also an increasing function of Δt , just like λ' in Equation (2). One then has to determine the ‘critical’ Δt where the asymptotic λ value is reached and use that value or the corresponding r_{1N} . It is the authors’ opinion that all measures, λ' , λ and r_{1N} , may be used when the critical time window is known, as representative of a lower and an upper bound as well as an intermediate estimate of jump length, to account for various complicated forms of molecular motion that may arise in the course of simulations or experiments.

As regards the implementation of the method, the two definitions in Equations (2) and (3) are combined in the following way. First, the curve of unweighted jumps with time is employed to obtain the time of jump occurrences. This is a smooth enough curve so that one can easily use it to identify the jumps as local maxima (elongated swarms), not only visually but also numerically. Then, the corresponding points of the curve of weighted jumps with time are sought in order to obtain the size of the jumps observed. The weighted size curve constitutes a rather noisy signal, due to the numerator in the weighting factor (Equation (3)), but thanks to its combined use with the unweighted one, this is not a problem. The r_{1N} curve can be used in the same way, i.e. once the time of jump occurrence is known, the corresponding end-to-end vector size is chosen.

3. Results and discussion

3.1. Macroscopic mass transport properties

In order to assess the results concerning the contribution of jumps to the overall diffusion, the methane self-diffusion coefficient, $D_{s,MSD}$, was calculated. The well-known Einstein formula, connecting the mean square displacement with time scales, was employed:

$$D_{s,MSD} = \lim_{\tau \rightarrow \infty} \frac{1}{6\tau} \left\langle \left| \mathbf{R}_i(t_0 + \tau) - \mathbf{R}_i(t_0) \right|^2 \right\rangle_{i,t_0}. \quad (5)$$

In the above equation, τ denotes the time scale and $\mathbf{R}_i(t)$ the position vector for the centre-of-mass of molecule i at time t . The brackets $\langle \rangle_{i,t_0}$ denote averaging with respect to all penetrant molecules i , and all initial times t_0 of every time interval equal to τ . Therefore, the quantity $\langle \left| \mathbf{R}_i(t_0 + \tau) - \mathbf{R}_i(t_0) \right|^2 \rangle_{i,t_0}$ corresponds to the penetrant’s mean square displacement (MSD). Results for each of the three structures simulated are shown in Figure 2. The linear part of the curves is easily

Table 1. Average size of diffusive jumps and their contribution to the total diffusivity. Results refer to independent simulations of the system studied, starting from three different initial configurations.

Initial system configuration:	1	2	3	St.	
	Average			dev.	
Jump length (Å)					
Equation (2)	5.08	4.82	5.18	5.03	0.19
Equation (3)	1.22	1.14	1.26	1.21	0.06
r_{1N}	2.25	2.11	2.26	2.21	0.08
Structure:	1	2	3	Average	St. dev.
Diffusivity ($\text{cm}^2 \text{s}^{-1} (\times 10^5)$)					
Equation (2)	6.53	5.94	6.80	6.42	0.44
Equation (3)	0.64	0.56	0.67	0.62	0.06
r_{1N}	2.45	2.15	2.45	2.35	0.17
Total (MSD)	10.19	9.84	12.86	10.96	1.65

observed and allows one to define self-diffusivity according to Equation (5). Table 1 summarizes self-diffusion coefficient values of the gas–liquid mixtures obtained from the present simulations, along with those based on the jumps’ contribution, as will be explained in the subsequent paragraphs. The average coefficient is found to be equal to $(1.10 \pm 0.16) \times 10^{-4} \text{cm}^2 \text{s}^{-1}$, an order of magnitude higher than the experimental value reported under similar conditions [32]. The overestimation can be attributed to the relatively small size of the polymer chains as compared with the molecular weights encountered in the real material, to the slightly lower density than that measured experimentally, and to the coarse-grained character of the united atom force-field employed, i.e. the absence of hydrogen atoms that would add a hindering or ‘friction’ effect to the molecular motion. However, given the approximations inherent in the analysis of the experimental data, the aforementioned value constitutes a fairly good result.

Following the original publication of the method [3], we have also estimated the anisotropy of the penetrants’ motion by means of the values of the displacement correlation matrix elements, normalized by the MSD. These are defined by

$$C_{\alpha\beta}(\tau) = \frac{\langle \Delta\alpha_i \Delta\beta_i \rangle_{i,t_0}}{\langle \Delta R_i^2 \rangle_{i,t_0}} - \frac{\delta_{\alpha\beta}}{3}, \quad (6)$$

where ΔR_i is the i th penetrant’s displacement averaged over all time scales τ , $\Delta\alpha_i$ is the corresponding displacement along the axis $\alpha=x,y,z$, and $\delta_{\alpha\beta}$ is Kronecker’s symbol. Values of the above elements close to zero for large time scales τ indicate isotropic

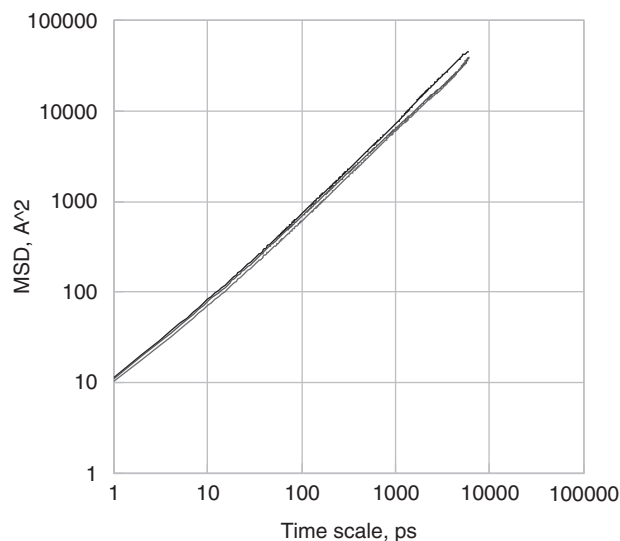


Figure 1. Mean square displacement (\AA^2) of methane dispersed in $n\text{-C}_{100}\text{H}_{202}$.

motion. The correlation matrix elements have been averaged over time scales that were employed in the calculation of diffusivity, i.e. excluding short ones that exhibit subdiffusing behavior as well as long ones, which are subject to larger statistical error as the respective time intervals become fewer. Neither significant anisotropy nor any strong correlation in the penetrants' motion along the x , y or z axis in any of the systems studied is inferred by the values computed, which hardly exceed 10% of the MSD in the time scales considered. The linearity of the curves shown in Figure 1 combined with the aforementioned lack of correlation corroborate that the normal diffusion regime has been attained within the space and time-scales studied.

As mentioned in Section 1, the obtained Einstein or MSD coefficients are a measure of the *overall* diffusive motion which is due to various microscopic mechanisms, either of jump-like nature or others. The contribution of a jump or hopping mechanism is analysed in the next subsection.

3.2. Microscopic diffusion mechanisms

Although visual representations of the penetrants' motion are not suitable for quantitative processing, they are helpful in clarifying the notions and assumptions made in the analysis of our results. Figure 2 shows a three-dimensional plot of a typical trajectory of a single methane molecule when periodic boundary conditions are removed. Three typical scenarios are clearly depicted in the figure. The part of the trajectory

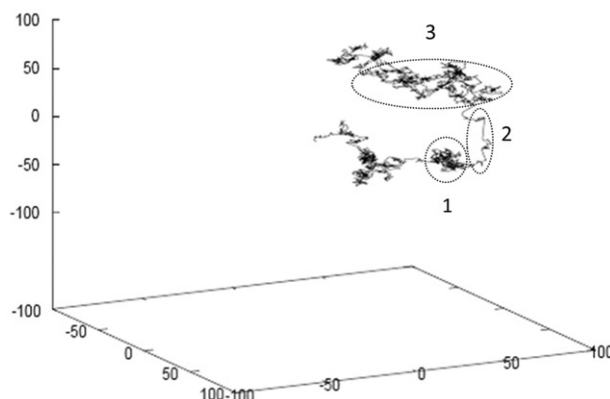


Figure 2. Three-dimensional plot of a single penetrant trajectory (periodic boundary conditions removed). 1=A 'blob' of points due to the penetrant being trapped in a rather stable cavity. 2=A rather fast displacement that may be identified as an inter-cavity 'jump'. 3=A more complicated displacement, possibly combining smooth penetrant translocation, the drifting effect of the polymer upon the penetrant, small jumps and intra-cavity motion.

indexed '1' corresponds to the motion of the particle when it is trapped in a cavity formed by the surrounding polymer molecules. Then, a kind of tunnel seems to be formed and the molecule travels rather fast to another region (index '2'). This can be considered a 'jump' event. Then the molecule settles in another cavity, but it does not stay there indefinitely. Rather, it follows a very complex path (index '3'), probably due to drifting motion caused by the polymer matrix, combined with the temporary formation of other cavities, small jumps therein, etc. It is obvious that jumps are not the sole contribution to the overall diffusive motion; however, they may constitute an important part thereof. Their quantitative treatment may help us better understand the way and the extent to which various heavy molecular weight materials allow lighter species to penetrate through them.

In search of the jump effect in our simulations, both unweighted and weighted jump lengths were calculated, according to the definitions given in Equations (2) and (3). Such curves are depicted in Figure 3 for two given time intervals Δt . As explained in the previous section, the unweighted curves serve the purpose of identifying the *time* when a jump takes place, namely the time a local maximum is encountered. Then, the corresponding value of the weighted curve is obtained as a measure of the real jump *size*. However, for the purpose of comparison, the corresponding length of the end-to-end vector of the points swarm was also calculated. Usually, the unweighted curves are smooth enough so that determination of

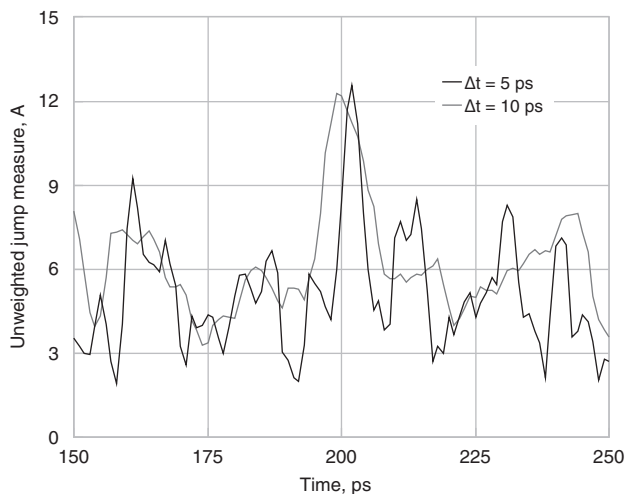


Figure 3. Identification of jumps of a single methane molecule diffusing through $n\text{-C}_{100}\text{H}_{202}$ via the ‘unweighted’ version of the jump detection method for different time windows Δt (5 and 10 ps).

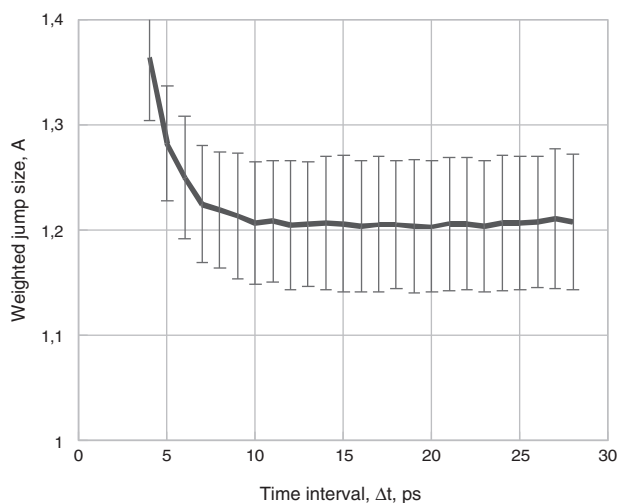


Figure 4. Weighted methane jump length, λ , averaged over all jumps observed in the three $n\text{-C}_{100}\text{H}_{202}$ structures studied, versus time interval Δt , clearly attains an asymptotic value for Δt larger than 10 ps.

local maxima is quite easy and can be done by tracking the change in slope in the form of the difference between two successive values. In some exceptional ‘noisy’ cases, moving averages of over 10 to 20 successive points had to be employed instead of the original curves.

As mentioned above, the weighting scheme allows one to remove the arbitrariness inherent in the introduction of an indeterminate time window Δt . Figure 4 shows the average weighted jump length with respect to time intervals Δt . The jump size reaches an

asymptotic value at small values of Δt , namely at Δt approximately equal to 10 ps, which is an indication that a random-walk character sets in at longer time intervals – for a detailed explanation, the reader is referred to the original publication of the method [3]. Table 1 summarizes the average jump lengths observed in all three systems for $\Delta t = 10$ ps, along with the respective diffusivities calculated on the basis of a random-walk model (Equation (4)). As already mentioned, three definitions of jump length are employed, namely those given by Equations (2) and (3) (unweighted and weighted lengths) and the size of the end-to-end vector of the observation points ‘swarm’ for the reasons explained in the theoretical section.

In agreement with what one would expect by visually inspecting the three-dimensional unfolded penetrant trajectories, such as that depicted in Figure 2, mechanisms other than jumps constitute the main contribution to the overall diffusion. Two of the measures employed provide a small value for the jumps’ contribution, amounting to more than 6% and probably around 14% of the total diffusivity, whereas a value close to 59%, based on the unweighted lengths, should be considered as an overestimation. However, the simplicity of our model does not allow one to draw conclusive results concerning the importance of such hopping mechanisms in heavy molecular weight systems. Therefore, a detailed investigation of larger systems of higher molecular weight and various architectures will be attempted in a subsequent work.

4. Conclusions

In this work, a method for the quantitative identification of individual penetrant jumps was applied to study the dynamics of a methane- $\text{C}_{100}\text{H}_{202}$ system via MD simulations. The method is based on the calculation of certain ‘size measures’ to identify individual jump events and quantify their contribution to the total diffusive motion observed. Data such as average jump lengths, frequency of their occurrence, etc. can easily be collected and help describe in detail the characteristics of the system’s behavior. By calculating a jump-induced diffusion coefficient and comparing it with the total diffusivity, e.g. that computed by the Einstein relation, one can determine to what extent diffusion is mainly due to such jump events or other microscopic mechanisms that are also active.

As in the original publication of the method [3] concerning systems of smaller molecular weight, in the present work it was also found that diffusive jumps are not the only mechanism present. Actually, other mechanisms, probably including drift by the

macromolecules upon the penetrant and gradual translation of the gas molecules themselves are more important. Two of the three measures employed, weighted jump size (Equation (3)) and the end-to-end vector of a set of observation points 'sliding' over the penetrant trajectory, suggest that the jumps' contribution amounts to about 6 to 14% of the total diffusivity. An estimate of 59% provided by the other measure, unweighted jump size (Equation (2)), should be considered as an upper bound and is clearly an overestimation for the reasons explained in the theoretical section of this article.

It would be of great interest to identify the other microscopic mechanisms underlying diffusion in the systems studied. One way to do this would be by investigating what changes take place when specific factors are eliminated. For instance, by decreasing the temperature, the polymer approaches its glassy state and the polymer matrix tends to be immobilized with only local vibrational modes being present. Therefore, no drifting due to polymer translational modes takes place and the jumps would be expected to contribute to a larger extent. On the other hand, such jumps would be less frequent as the polymer's thermal motion would only rarely allow for inter-cavity translocations, thus resulting in significantly reduced overall diffusivity. Computations at lower temperatures are underway in order to address the temperature dependence question in a forthcoming article. This and the present study will constitute the preliminary steps of a wider research program that will investigate systems of light substances dispersed in matrices of higher molecular weight and various architectures. Quantitative measures for the classification and characterization of other mass transport microscopic mechanisms will also be attempted.

Acknowledgements

The authors wish to thank the anonymous reviewer of the present work for his/her fruitful comments and suggestions. The computer time allocation at the facilities of the Computer Centre of the National and Kapodistrian University of Athens is also gratefully acknowledged.

References

[1] F.P. Ricci and D. Rocca, in *Molecular Liquids: Dynamics and Interactions*, edited by A.J. Barnes, W.J. Orville Thomas and J. Jarwood (NATO ASI, Vol. C 135) (Reidel, Dordrecht, 1984), pp. 35–58.

[2] H. Zheng, S. Claridge, A. Minor, A.P. Alivisatos and U. Dahmen, *Nano Lett.* **9**, 2460 (2009).

[3] T.E. Raptis, V.E. Raptis and J. Samios, *J. Phys. Chem.* **111**, 13683 (2007).

[4] J. Sonnenburg, J. Gao and J.H. Weiner, *Macromolecules* **23**, 4653 (1990).

[5] H. Takeuchi, *J. Chem. Phys.* **93**, 2062 (1990).

[6] H. Takeuchi, *J. Chem. Phys.* **93**, 4490 (1990).

[7] F. Müller-Plathe, S.C. Rogers and W.F. van Gunsteren, *Chem. Phys. Lett.* **199**, 237 (1992).

[8] F. Müller-Plathe, *J. Chem. Phys.* **94**, 3192 (1991).

[9] F. Müller-Plathe, *J. Chem. Phys.* **96**, 3200 (1992).

[10] R.M. Sok, H.J.C. Berendsen and W.F. van Gunsteren, *Chem. Phys.* **96**, 4699 (1992).

[11] P.V.K. Pant and R.H. Boyd, *Macromolecules* **26**, 679 (1993).

[12] A.A. Gusev, F. Müller-Plathe, W.R. van Gunsteren and U.W. Suter, *Adv. Polym. Sci.* **116**, 207 (1994).

[13] H. Takeuchi and K. Okazaki, *Kobunshi Ronbunshu* **51**, 387 (1994).

[14] C.S. Chassapis, J.K. Petrou, J.H. Petropoulos and D.N. Theodorou, *Macromolecules* **29**, 3615 (1996).

[15] F. Müller-Plathe, *J. Membr. Sci.* **141**, 147 (1998).

[16] O. Hahn, D.A. Mooney, F. Müller-Plathe and K. Kremer, *J. Chem. Phys.* **111**, 6061 (1999).

[17] D.A. Mooney and J.M.D. MacElroy, *J. Chem. Phys.* **110**, 11087 (1999).

[18] E. Tocci, D. Hofmann, D. Paul, N. Russo and E. Drioli, *Polymer* **42**, 521 (2001).

[19] S. Neyertz and D. Brown, *Macromolecules* **37**, 10109 (2004).

[20] D. Pavel and S. Shanks, *Polymer* **46**, 6135 (2005).

[21] A. Striolo, C. McCabe and P.T. Cummings, *Macromolecules* **38**, 8950 (2005).

[22] A. Striolo, C. McCabe and P.T. Cummings, *J. Phys. Chem. B* **109**, 14300 (2005).

[23] M. Meunier, *J. Chem. Phys.* **123**, 134906 (2005).

[24] K.L. Tung and K.T. Lu, *J. Membr. Sci.* **272**, 37 (2006).

[25] E. Smit, M.H.V. Mulder, C.A. Smolders, H. Karrenbeld, J. van Eerden and D. Feil, *J. Membr. Sci.* **73**, 247 (1992).

[26] R. Chang and A. Yethiraj, *Phys. Rev. Lett.* **96**, 107802 (2006).

[27] J.F. Vega, S. Rastogi, G.W.M. Peters and H.E.H. Meijer, *J. Rheol.* **48**, 663 (2004).

[28] S.K. Nath, F.A. Escobedo and J.J. de Pablo, *J. Chem. Phys.* **108**, 9905 (1998).

[29] M.G. Martin and J.I. Siepmann, *J. Phys. Chem. B* **102**, 2569 (1998).

[30] U. Gaur and B. Wunderlich, *J. Phys. Chem. Ref. Data* **10**, 119 (1981).

[31] S. Chandrasekhar, *Rev. Mod. Phys.* **15**, 1 (1943).

[32] A.S. Michaels and H.J. Bixler, *J. Polym. Sci.* **10**, 413 (1961).